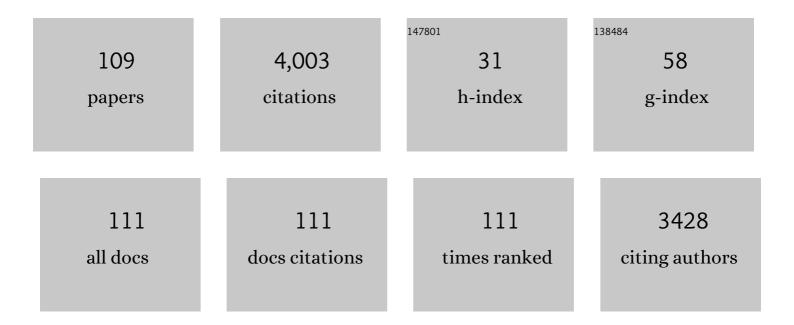
List of Publications by Year in descending order

Source: https://exaly.com/author-pdf/2256025/publications.pdf Version: 2024-02-01



#	Article	IF	CITATIONS
1	Disentangling the Impact of Global and Regional Climate Changes During the Middle Eocene in the Hampshire Basin: New Insights From Carbonate Clumped Isotopes and Ostracod Assemblages. Paleoceanography and Paleoclimatology, 2022, 37, .	2.9	6
2	Determination of the spatial distribution of wetting in the pore networks of rocks. Journal of Colloid and Interface Science, 2022, 613, 786-795.	9.4	17
3	Origin and distribution of calcite cements in a folded fluvial succession: The Puigâ€reig anticline (southâ€eastern Pyrenees). Sedimentology, 2022, 69, 2319-2347.	3.1	7
4	Cenozoic sediment bypass versus Laramide exhumation and erosion of the Eagle Ford Group: Perspective from modelling of organic and inorganic proxy data (Maverick Basin, Texas, USA). Geology, 2022, 50, 817-821.	4.4	7
5	Stratigraphic evolutionÂand karstification of a Cretaceous Midâ€Pacific atoll (Resolution Guyot) resolved from coreâ€logâ€seismic integration and comparison with modern and ancient analogues. Basin Research, 2022, 34, 1536-1566.	2.7	2
6	Changing surface ocean circulation caused the local demise of echinoid Scaphechinus mirabilis in Taiwan during the Pleistocene–Holocene transition. Scientific Reports, 2022, 12, 8204.	3.3	1
7	Towards a new understanding of the genesis of chalk: Diagenetic origin of micarbs confirmed by clumped isotope analysis. Sedimentology, 2021, 68, 513-530.	3.1	17
8	Constraining stratal architecture and pressure barriers in the subsalt Karachaganak Carboniferous carbonate platforms using forward stratigraphic modelling. Marine and Petroleum Geology, 2021, 124, 104771.	3.3	3
9	Combining clumped isotope and trace element analysis to constrain potential kinetic effects in calcite. Geochimica Et Cosmochimica Acta, 2021, 296, 117-130.	3.9	3
10	A Unified Clumped Isotope Thermometer Calibration (0.5–1,100°C) Using Carbonateâ€Based Standardization. Geophysical Research Letters, 2021, 48, e2020GL092069.	4.0	116
11	InterCarb: A Community Effort to Improve Interlaboratory Standardization of the Carbonate Clumped Isotope Thermometer Using Carbonate Standards. Geochemistry, Geophysics, Geosystems, 2021, 22, e2020GC009588.	2.5	110
12	Multiple fluid flow events from saltâ€related rifting to basin inversion (Upper Pedraforca thrust sheet,) Tj ETQqO	0 Q.rgBT /0	Overlock 10 12
13	Evidence of taxonomic non-equilibrium effects in the clumped isotope composition of modern cephalopod carbonate. Chemical Geology, 2021, 578, 120317.	3.3	9
14	The Sensitivity of Estimates of Multiphase Fluid and Solid Properties of Porous Rocks to Image Processing. Transport in Porous Media, 2020, 131, 985-1005.	2.6	43
15	Fluid Dynamics in a Thrust Fault Inferred from Petrology and Geochemistry of Calcite Veins: An Example from the Southern Pyrenees. Geofluids, 2020, 2020, 1-25.	0.7	12
16	Geostatistical Earth modeling of cyclic depositional facies and diagenesis. AAPG Bulletin, 2020, 104, 711-734.	1.5	2
17	From hydroplastic to brittle deformation: Controls on fluid flow in fold and thrust belts. Insights from the Lower Pedraforca thrust sheet (SE Pyrenees). Marine and Petroleum Geology, 2020, 120, 104517.	3.3	16

18Geochronological and geochemical data from fracture-filling calcites from the Lower Pedraforca1.0018thrust sheet (SE Pyrenees). Data in Brief, 2020, 31, 105896.1.00

#	Article	IF	CITATIONS
19	Significance of Fracture-Filling Rose-Like Calcite Crystal Clusters in the SE Pyrenees. Minerals (Basel,) Tj ETQq1	1 0.78431 2.0	4 rgBT /Over
20	Early dolomitization and partial burial recrystallization: a case study of Middle Triassic peritidal dolomites in the Villány Hills (SW Hungary) using petrography, carbon, oxygen, strontium and clumped isotope data. International Journal of Earth Sciences, 2020, 109, 1051-1070.	1.8	12
21	Fluid Surface Coverage Showing the Controls of Rock Mineralogy on the Wetting State. Geophysical Research Letters, 2020, 47, e2019GL086380.	4.0	32
22	Effects of oxygen plasma ashing treatment on carbonate clumped isotopes. Rapid Communications in Mass Spectrometry, 2020, 34, e8802.	1.5	12
23	Regional-scale paleofluid system across the Tuscan Nappe–Umbria–Marche Apennine Ridge (northern) Tj E Earth, 2020, 11, 1617-1641.	TQq1 1 0.7 2.8	784314 rgBT 23
24	Influence of basement rocks on fluid evolution during multiphase deformation: the example of the Estamariu thrust in the Pyrenean Axial Zone. Solid Earth, 2020, 11, 2257-2281.	2.8	5
25	Clumped-isotope palaeothermometry and LA-ICP-MS U–Pb dating of lava-pile hydrothermal calcite veins. Contributions To Mineralogy and Petrology, 2019, 174, 1.	3.1	34
26	Tropical temperature in the Maastrichtian Danish Basin: Data from coccolith Δ47 and δ180. Geology, 2019, 47, 1074-1078.	4.4	11
27	Benthic foraminiferal biotic events related to the Paleocene–Eocene Thermal Maximum along the California margin. Marine Micropaleontology, 2019, 150, 101745.	1.2	1
28	Effects of Improved ¹⁷ O Correction on Interlaboratory Agreement in Clumped Isotope Calibrations, Estimates of Mineral‧pecific Offsets, and Temperature Dependence of Acid Digestion Fractionation. Geochemistry, Geophysics, Geosystems, 2019, 20, 3495-3519.	2.5	134
29	Rock-buffered recrystallization of Marion Plateau dolomites at low temperature evidenced by clumped isotope thermometry and X-ray diffraction analysis. Geochimica Et Cosmochimica Acta, 2019, 252, 190-212.	3.9	39
30	From Early Contraction to Post-Folding Fluid Evolution in the Frontal Part of the Bóixols Thrust Sheet (Southern Pyrenees) as Revealed by the Texture and Geochemistry of Calcite Cements. Minerals (Basel, Switzerland), 2019, 9, 117.	2.0	18
31	Multi-phase dolomitization and recrystallization of Middle Triassic shallow marine–peritidal carbonates from the Mecsek Mts. (SW Hungary), as inferred from petrography, carbon, oxygen, strontium and clumped isotope data. Marine and Petroleum Geology, 2019, 101, 440-458.	3.3	20
32	The clumped (13C18O) isotope composition of echinoid calcite: Further evidence for "vital effects―in the clumped isotope proxy. Geochimica Et Cosmochimica Acta, 2019, 245, 172-189.	3.9	40
33	Quantitative controls on the regional geometries and heterogeneities of the Rayda to Shu'aiba formations (Northern Oman) using forward stratigraphic modelling. Marine and Petroleum Geology, 2019, 99, 45-60.	3.3	8
34	Burial estimates constrained by clumped isotope thermometry: example of the Lower Cretaceous Qishn Formation (Haushi-Huqf High, Oman). Geological Society Special Publication, 2018, 435, 107-121.	1.3	14
35	Ground-based hyperspectral imaging as a tool to identify different carbonate phases in natural cliffs. International Journal of Remote Sensing, 2018, 39, 4088-4114.	2.9	11
36	Deciphering the State of the Late Miocene to Early Pliocene Equatorial Pacific. Paleoceanography and Paleoclimatology, 2018, 33, 246-263.	2.9	30

#	Article	IF	CITATIONS
37	Evolution of hot fluids in the Chingshui geothermal field inferred from crystal morphology and geochemical vein data. Geothermics, 2018, 74, 305-318.	3.4	14
38	A new approach to geobarometry by combining fluid inclusion and clumped isotope thermometry in hydrothermal carbonates. Terra Nova, 2018, 30, 199-206.	2.1	23
39	Controls on the formation of stratabound dolostone bodies, Hammam Faraun Fault block, Gulf of Suez. Sedimentology, 2018, 65, 1973-2002.	3.1	24
40	Testing clumped isotopes as a reservoir characterization tool: a comparison with fluid inclusions in a dolomitized sedimentary carbonate reservoir buried to 2–4 km. Geological Society Special Publication, 2018, 468, 189-202.	1.3	17
41	Geostatistical Modelling of Cyclic and Rhythmic Facies Architectures. Mathematical Geosciences, 2018, 50, 609-637.	2.4	11
42	Assessment of Factors Controlling Clumped Isotopes and δ ¹⁸ 0 Values of Hydrothermal Vent Calcites. Geochemistry, Geophysics, Geosystems, 2018, 19, 1844-1858.	2.5	12
43	Geometry, spatial arrangement and origin of carbonate grainâ€dominated, scourâ€fill and eventâ€bed deposits: Late Jurassic Jubaila Formation and Arabâ€D Member, Saudi Arabia. Sedimentology, 2018, 65, 1043-1066.	3.1	13
44	Changes in fluid regime in syn-orogenic sediments during the growth of the south Pyrenean fold and thrust belt. Global and Planetary Change, 2018, 171, 207-224.	3.5	30
45	Mental health in the field. Nature Geoscience, 2018, 11, 618-620.	12.9	23
46	Magmatic-like fluid source of the Chingshui geothermal field, NE Taiwan evidenced by carbonate clumped-isotope paleothermometry. Journal of Asian Earth Sciences, 2017, 149, 124-133.	2.3	15
47	Reducing contamination parameters for clumped isotope analysis: The effect of lowering Porapakâ"¢ Q trap temperature to below –50°C. Rapid Communications in Mass Spectrometry, 2017, 31, 1313-1323.	1.5	21
48	Development of an equatorial carbonate platform across the Triassic-Jurassic boundary and links to global palaeoenvironmental changes (Musandam Peninsula, UAE/Oman). Gondwana Research, 2017, 45, 100-117.	6.0	9
49	Late Miocene climate and time scale reconciliation: Accurate orbital calibration from a deep-sea perspective. Earth and Planetary Science Letters, 2017, 475, 254-266.	4.4	41
50	Assessing and calibrating the ATR-FTIR approach as a carbonate rock characterization tool. Sedimentary Geology, 2017, 347, 36-52.	2.1	47
51	Modelling Asymmetrical Facies Successions Using Pluri-Gaussian Simulations. Quantitative Geology and Geostatistics, 2017, , 59-75.	0.1	6
52	Relationship between karstification and burial dolomitization in Permian platform carbonates (Lower) Tj ETQq0 C) 0 ₂₉ BT /C	overlock 107
53	Paired stable isotopes (O, C) and clumped isotope thermometry of magnesite and silica veins in the New Caledonia Peridotite Nappe. Geochimica Et Cosmochimica Acta, 2016, 183, 234-249.	3.9	33

54Exploring the potential of clumped isotope thermometry on coccolithâ€rich sediments as a sea surface
temperature proxy. Geochemistry, Geophysics, Geosystems, 2016, 17, 4092-4104.2.511

#	Article	IF	CITATIONS
55	Clumped-isotope thermometry of magnesium carbonates in ultramafic rocks. Geochimica Et Cosmochimica Acta, 2016, 193, 222-250.	3.9	38

56 Crestal graben fluid evolution during growth of the Puig-reig anticline (South Pyrenean fold and) Tj ETQq0 0 0 rgBT 10 rf 50 7

57	Evaluating climatic response to external radiative forcing during the late Miocene to early Pliocene: New perspectives from eastern equatorial Pacific (IODP U1338) and North Atlantic (ODP 982) locations. Paleoceanography, 2016, 31, 167-184.	3.0	31
58	Community software for challenging isotope analysis: First applications of â€~Easotope' to clumped isotopes. Rapid Communications in Mass Spectrometry, 2016, 30, 2285-2300.	1.5	156
59	Building More Realistic 3-D Facies Indicator Models. , 2016, , .		2

60 Detailed 3-D depositional architecture of Late Jurassic carbonate–anhydrite cycles (Brightling Mine,) Tj ETQq0 0 0.3gBT /Overlock 10 Tr

61	Dolomitization Processes in Hydrocarbon Reservoirs: Insight from Geothermometry Using Clumped Isotopes. Procedia Earth and Planetary Science, 2015, 13, 265-268.	0.6	10
62	Inter-Well Scale Sedimentological Heterogeneities And Facies Architecture Of Upper Jurassic Carbonate Reservoir And Anhydrite Seals: Lessons Learned Using Outcrop Analogues. , 2015, , .		0
63	Hyperspectral Remote Sensing for the Characterization of Dolomite Bodies: A Case Study in the Central Oman Mountains - Lower Khuff Analogue. , 2015, , .		0
64	Technical Note: A simple method for vaterite precipitation for isotopic studies: implications for bulk and clumped isotope analysis. Biogeosciences, 2015, 12, 3289-3299.	3.3	7
65	Exploring the geological features and processes that control the shape and internal fabrics of late diagenetic dolomite bodies (Lower Khuff equivalent – Central Oman Mountains). Marine and Petroleum Geology, 2015, 68, 325-340.	3.3	22
66	Temperature dependence of oxygen- and clumped isotope fractionation in carbonates: A study of travertines and tufas in the 6–95°C temperature range. Geochimica Et Cosmochimica Acta, 2015, 168, 172-192.	3.9	199
67	Diagenesis of phosphatic hardgrounds in the Monterey Formation: A perspective from bulk and clumped isotope geochemistry. Bulletin of the Geological Society of America, 2015, 127, 1453-1463.	3.3	9
68	Effects of brine chemistry and polymorphism on clumped isotopes revealed by laboratory precipitation of mono- and multiphase calcium carbonates. Geochimica Et Cosmochimica Acta, 2015, 160, 155-168.	3.9	21
69	Diagenetic Geobodies: Fracture-Controlled Burial Dolomite in Outcrops From Northern Oman. SPE Reservoir Evaluation and Engineering, 2015, 18, 84-93.	1.8	11
70	Laboratory calibration of the calcium carbonate clumped isotope thermometer in the 25–250 °C temperature range. Geochimica Et Cosmochimica Acta, 2015, 157, 213-227.	3.9	133
71	Sedimentological and isotopic heterogeneities within a Jurassic carbonate ramp (UAE) and implications for reservoirs in the Middle East. Marine and Petroleum Geology, 2015, 68, 240-257.	3.3	19
72	Application of redox sensitive proxies and carbonate clumped isotopes to Mesozoic and Palaeozoic radiaxial fibrous calcite cements. Chemical Geology, 2015, 417, 306-321.	3.3	28

#	Article	IF	CITATIONS
73	Urban flood vulnerability zoning of Cochin City, southwest coast of India, using remote sensing and GIS. Natural Hazards, 2015, 75, 1271-1286.	3.4	76
74	The magnesium isotope (δ26Mg) signature of dolomites. Geochimica Et Cosmochimica Acta, 2015, 149, 131-151.	3.9	125
75	Dolomitization of Lower Cretaceous Peritidal Carbonates By Modified Seawater: Constraints From Clumped Isotopic Paleothermometry, Elemental Chemistry, and Strontium Isotopes. Journal of Sedimentary Research, 2014, 84, 552-566.	1.6	30
76	Dimensions, texture-distribution, and geochemical heterogeneities of fracture–related dolomite geobodies hosted in Ediacaran limestones, northern Oman. AAPG Bulletin, 2014, 98, 1789-1809.	1.5	14
77	Interaction of stratigraphic and sedimentological heterogeneities with flow in carbonate ramp reservoirs: impact of fluid properties and production strategy. Petroleum Geoscience, 2014, 20, 7-26.	1.5	15
78	Time-capsule concretions: Unlocking burial diagenetic processes in the Mancos Shale using carbonate clumped isotopes. Earth and Planetary Science Letters, 2014, 394, 30-37.	4.4	102
79	Carbonate Reservoir Analogues and Clumped Isotopes: How Combined Geometries and Geochemistry of Outcrops Help Reservoir Management in the Middle East. , 2014, , .		2
80	Diagenetic Geobodies: Fracture-Controlled Burial Dolomite Bodies in Outcrops from Northern Oman. , 2014, , .		0
81	Interplay between depositional facies, diagenesis and early fractures in the Early Cretaceous Habshan Formation, Jebel Madar, Oman. Marine and Petroleum Geology, 2013, 43, 489-503.	3.3	22
82	Linking process, dimension, texture, and geochemistry in dolomite geobodies: A case study from Wadi Mistal (northern Oman). AAPG Bulletin, 2013, 97, 1181-1207.	1.5	29
83	Impact of dynamic sedimentation on facies heterogeneities in Lower Cretaceous peritidal deposits of central east Oman. Sedimentology, 2013, 60, 1156-1183.	3.1	15
84	Diagenetic Implications of Stylolitization In Pelagic Carbonates, Canterbury Basin, Offshore New Zealand. Journal of Sedimentary Research, 2013, 83, 226-240.	1.6	36
85	Clay assemblage and oxygen isotopic constraints on the weathering response to the Paleocene-Eocene the response to the Paleocene-Eocene thermal maximum, east coast of North America. Geology, 2012, 40, 591-594.	4.4	53
86	Influence of climate and dolomite composition on dedolomitization: insights from a multi-proxy study in the central Oman Mountains. Journal of Sedimentary Research, 2012, 82, 177-195.	1.6	38
87	Access to Antigens Related to Anthrose Using Pivotal Cyclic Sulfite/Sulfate Intermediates. Journal of Organic Chemistry, 2011, 76, 5985-5998.	3.2	7
88	Timing and magnitude of Miocene eustasy derived from the mixed siliciclastic-carbonate stratigraphic record of the northeastern Australian margin. Earth and Planetary Science Letters, 2011, 304, 455-467.	4.4	103
89	Floating islands in a tropical wetland of peninsular India. Wetlands Ecology and Management, 2009, 17, 641-653.	1.5	23
90	North American continental margin records of the Paleoceneâ€Eocene thermal maximum: Implications for global carbon and hydrological cycling. Paleoceanography, 2008, 23, .	3.0	176

#	Article	IF	CITATIONS
91	Pore pressure penetrometers document high overpressure near the seafloor where multiple submarine landslides have occurred on the continental slope, offshore Louisiana, Gulf of Mexico. Earth and Planetary Science Letters, 2008, 269, 309-325.	4.4	105
92	Eustatic variations during the Paleocene $\hat{a} {\in} E$ ocene greenhouse world. Paleoceanography, 2008, 23, .	3.0	167
93	Erratum to "Pore pressure penetrometers document high overpressure near the seafloor where multiple submarine landslides have occurred on the continental slope, offshore Louisiana, Gulf of Mexico" [Earth and Planetary Science Letters 269/3-4 (2008) 309-32]. Earth and Planetary Science Letters, 2008, 274, 269-283.	4.4	37
94	The Palaeocene–Eocene carbon isotope excursion: constraints from individual shell planktonic foraminifer records. Philosophical Transactions Series A, Mathematical, Physical, and Engineering Sciences, 2007, 365, 1829-1842.	3.4	102
95	Environmental precursors to rapid light carbon injection at the Palaeocene/Eocene boundary. Nature, 2007, 450, 1218-1221.	27.8	296
96	Regional trends in clay mineral fluxes to the Queensland margin and ties to middle Miocene global cooling. Palaeogeography, Palaeoclimatology, Palaeoecology, 2006, 233, 204-224.	2.3	10
97	Chemostratigraphy in Miocene heterozoan carbonate settings: applications, limitations and perspectives. Geological Society Special Publication, 2006, 255, 307-322.	1.3	19
98	Relative Control of Paleoceanography, Climate, and Eustasy over Heterozoan Carbonates: A Perspective from Slope Sediments of the Marion Plateau (ODP LEG 194). Journal of Sedimentary Research, 2005, 75, 216-230.	1.6	22
99	Phosphogenesis and organic-carbon preservation in the Miocene Monterey Formation at Naples Beach, California—The Monterey hypothesis revisited. Bulletin of the Geological Society of America, 2005, 117, 589.	3.3	78
100	Plotting and analyzing data trends in ternary diagrams made easy. Eos, 2004, 85, 158-158.	0.1	11
101	δ180 and Marion Plateau backstripping: Combining two approaches to constrain late middle Miocene eustatic amplitude. Geology, 2004, 32, 829.	4.4	80
102	Mixed carbonate-siliciclastic record on the North African margin (Malta)—coupling of weathering processes and mid Miocene climate. Bulletin of the Geological Society of America, 2003, 115, 217-229.	3.3	91
103	Carbonaceous and Phosphate-Rich Sediments of the Miocene Monterey Formation at El Capitan State Beach, California, U.S.A Journal of Sedimentary Research, 2002, 72, 252-267.	1.6	31
104	XPS and TOF-SIMS Microanalysis of a Peptide/Polymer Drug Delivery Device. Analytical Chemistry, 1995, 67, 3871-3878.	6.5	16
105	The structural basis for pyocin resistance in Neisseria gonorrhoeae lipooligosaccharides. Journal of Biological Chemistry, 1991, 266, 19303-11.	3.4	105
106	Amino and hydrazino alkyl benzoates as derivatizing agents for the separation and mass spectrometric analysis of oligosaccharides from bacterial lipooligosaccharides. Analytical Biochemistry, 1990, 187, 281-291.	2.4	24
107	Integration of multispectral satellite and hyperspectral field data for aquatic macrophyte studies. International Archives of the Photogrammetry, Remote Sensing and Spatial Information Sciences - ISPRS Archives, 0, XL-8, 581-588.	0.2	7
108	Rapid Sedimentation, Overpressure, and Focused Fluid Flow, Gulf of Mexico Continental Margin. Scientific Drilling, 0, 3, 12-17.	0.6	19

#	Article	IF	CITATIONS
109	Development of a web geoservices platform for School of Environmental Sciences, Mahatma Gandhi University, Kerala, India. International Archives of the Photogrammetry, Remote Sensing and Spatial Information Sciences - ISPRS Archives, 0, XL-8, 1207-1212.	0.2	0